© 2018. Published by The Company of Biologists Ltd | Journal of Cell Science (2018) 131, jcs210906. doi:10.1242/jcs.210906

RESEARCH ARTICLE

BAMBI is a novel HIF1-dependent modulator of TGFβ-mediated disruption of cell polarity during hypoxia

Irina Raykhel[1], Fazeh Moafi[1], Satu M. Myllymäki[1,*], Patricia G. Greciano[2], Karl S. Matlin[2], Jose V. Moyano[2], Aki Manninen[1,‡] and Johanna Myllyharju[1,‡,§]

ABSTRACT

Hypoxia and loss of cell polarity are common features of malignant carcinomas. Hypoxia-inducible factor 1 (HIF1) is the major regulator of cellular hypoxia response and mediates the activation of ∼300 genes. Increased HIF1 signaling is known to be associated with epithelial–mesenchymal transformation. Here, we report that hypoxia disrupts polarized epithelial morphogenesis of MDCK cells in a HIF1α-dependent manner by modulating the transforming growth factor-β (TGFβ) signaling pathway. Analysis of potential HIF1 targets in the TGFβ pathway identified the bone morphogenetic protein and activin membrane-bound inhibitor (BAMBI), a transmembrane glycoprotein related to the type I receptors of the TGFβ family, whose expression was essentially lost in HIF1-depleted cells. Similar to what was observed in HIF1-deficient cells, BAMBI-depleted cells failed to efficiently activate TGFβ signaling and retained epithelial polarity during hypoxia. Taken together, we show that hypoxic conditions promote TGFβ signaling in a HIF1-dependent manner and BAMBI is identified in this pathway as a novel HIF1-regulated gene that contributes to hypoxia-induced loss of epithelial polarity.

KEY WORDS: BAMBI, Polarity, Hypoxia, TGFβ pathway, HIF1

INTRODUCTION

Hypoxia-inducible factors (HIFs) are transcription factors that facilitate adaptation to oxygen deprivation by activating ∼300 genes involved in erythropoiesis, angiogenesis, anaerobic metabolism, and cell differentiation and survival. HIFs are αβ heterodimers and the stability of the α-subunit is regulated by oxygen-dependent prolyl hydroxylation catalyzed by HIF prolyl 4-hydroxylases (HIF-P4Hs, also known as PHDs and EGLNs) (Kaelin and Ratcliffe, 2008; Myllyharju, 2013; Semenza, 2012). In normoxic conditions, HIF-P4Hs hydroxylate the HIFα subunit, which facilitates binding of the von Hippel–Lindau (VHL) E3 ubiquitin ligase complex and results in subsequent proteasomal degradation of HIFα. Under hypoxic conditions, however, HIF-P4Hs are inhibited allowing formation of the active HIFαβ heterodimer. Three HIFα isoforms exist in humans, with HIF1α and HIF2α being the main regulators of hypoxia target genes with at least partially non-overlapping functions (Keith et al., 2011; Koh and Powis, 2012; Schödel et al., 2013).

Reduced oxygen supply and increased HIF signaling is associated with different pathologies, including fibrosis and cancer (Higgins et al., 2008; Semenza, 2012). Intratumoral hypoxia is a common feature of the microenvironment of solid tumors of different origin, and overexpression of HIF is a sign of tumors that are highly resistant to chemo- and radiotherapy and have increased risk of metastasis (Vaupel and Mayer, 2007). Epithelial–mesenchymal transformation (EMT) is a physiological event in tissue development and regeneration, but promotes metastasis of malignant cells and contributes to the pathogenesis of tissue fibrosis (Higgins et al., 2008; Massagué, 2012; Rankin and Giaccia, 2016; Ruthenborg et al., 2014). Increased HIF signaling has been shown to induce EMT in several cell types either by directly regulating certain key EMT transcription factors or by indirectly affecting other cell signaling pathways such as, for example, Notch and transforming growth factor-β (TGFβ) pathways (Rankin and Giaccia, 2016).

TGFβ signaling can promote tumor growth, invasion and metastasis, and elevated TGFβ expression correlates with tissue fibrosis (Arjaans et al., 2012; Higgins et al., 2008; Massagué, 2012). However, TGFβ also has an opposite physiological role, and it is required for the maintenance of tissue homeostasis and suppression of tumor progression and can act as a tumor suppressor in premalignant cells (Arjaans et al., 2012; Massagué, 2012). The human TGFβ family includes over 30 members, which can be divided into two subfamilies: the TGFβ–activin–Nodal subfamily and the bone morphogenetic protein (BMP) subfamily (Massagué, 2012). TGFβ receptors are heterotetramers consisting of two TGFβ type I receptors (TGFβR1) and two TGFβ type II receptors (TGFβR2) (Massagué, 2012). TGFβ type III receptor (TGFβR3), also known as betaglycan, functions as a coreceptor with the other members of TGFβ receptor superfamily (Jovanović et al., 2016). TGFβ binds to TGFβR2 and recruits TGFβR1, which leads to TGFβR2-mediated phosphorylation and activation of TGFβR1. TGFβR1 then phosphorylates receptor-bound Smad transcription factors (Smad2/3), which form a complex with Smad4 and translocate to the nucleus, where they regulate the expression of ∼300 target genes (Massagué and Gomis, 2006). TGFβ itself is secreted from cells as part of a large latent complex that consists of latency-associated peptide (LAP) and one of the latent TGFβ-binding proteins (LTBPs) (Robertson and Rifkin, 2013). Therefore, TGFβ needs to be activated by releasing it from the latent complex before it can bind its receptor. Active TGFβ can be released from the latent complex by protease-mediated processing or by integrin-mediated mechanical disruption of the LAP–TGFβ interaction (Arjaans et al., 2012).

[1]Oulu Center for Cell-Matrix Research, Biocenter Oulu, Faculty of Biochemistry and Molecular Medicine, University of Oulu, 90220 Oulu, Finland. [2]Department of Surgery (Section of Research), University of Chicago, Chicago, IL 60637-1470, USA. *Present address: Developmental Biology Program, Institute of Biotechnology, University of Helsinki, 00014 Helsinki, Finland. ‡These authors contributed equally to this work

§Author for correspondence (johanna.myllyharju@oulu.fi)

K.S.M., 0000-0002-1251-0580; J.V.M., 0000-0003-1009-8059; A.M., 0000-0002-6263-8101; J.M., 0000-0001-7772-1250

Received 12 September 2017; Accepted 17 April 2018

Journal of Cell Science (2018) 131, jcs210906. doi:10.1242/jcs.210906

HIF and Smad-binding sites are frequently found close to each other in the regulatory regions of the target genes, suggesting a possible cooperative gene regulation by hypoxia and TGFβ signaling (Ruthenborg et al., 2014). Whether hypoxia and HIF-mediated signaling regulate epithelial cell polarity has not been thoroughly addressed. Here, we have studied this by using a well-characterized three-dimensional (3D) Madin–Darby canine kidney (MDCK) epithelial cell culture system, and show that HIF1 promotes TGFβ signaling, which, in turn, disrupts the formation of polarized MDCK cysts. Furthermore, we identify BAMBI as a novel mediator of HIF1-driven activation of TGFβ signaling and show that inactivation of BAMBI rescues MDCK cystogenesis during hypoxia.

RESULTS

Morphogenesis of MDCK cysts is perturbed during hypoxia in a HIF1α-dependent manner

To study the role of HIF1α in the cystogenesis of MDCK cells, we generated three independent HIF1α-knockdown (KD) MDCK cell lines by using a retrovirus-mediated RNA interference (RNAi) methodology (Manninen et al., 2005; Schuck et al., 2004). Efficient silencing, ranging from 65% to 95%, of the target HIF1α (*HIF1A*) mRNA was confirmed by quantitative real-time PCR (qRT-PCR) (Fig. 1A; Table S1). In accordance with the HIF1α mRNA depletion, the HIF1α protein level was reduced in the HIF1α-KD cell lines under hypoxic conditions when compared with wild-type (WT) control cells (Fig. 1A,B). All following experiments were

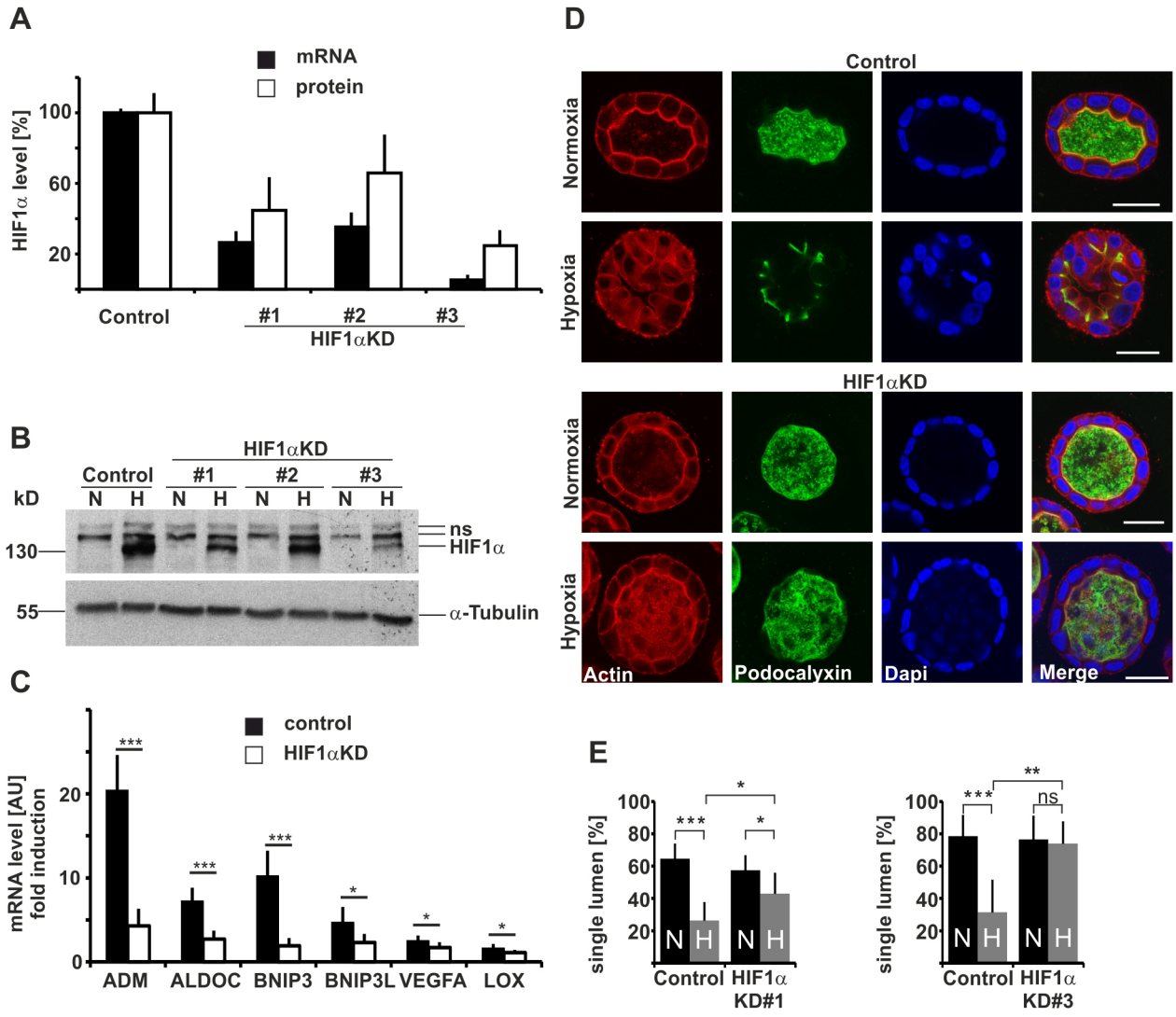

Fig. 1. Hypoxia leads to disrupted morphogenesis of MDCK cysts. (A–C) Control and three independent HIF1α-KD (#1, #2 and #3) MDCK cell lines were grown in 2D in normoxic (N) and hypoxic (H, 24 h 1% O_2) conditions. (A) Expression of HIF1α mRNA in normoxia was analyzed by qRT-PCR analysis. Data are presented as mean±s.d., n=11. A quantification of the HIF1α protein amount during hypoxia, from experiments as shown in B, is also shown, n=3. (B) A representative HIF1α western blot of control and the HIF1α-KD MDCK cell lines. α-tubulin is shown as a loading control. (C) qRT-PCR analysis of the mRNA expression level of selected HIF target genes in 2D cultures of control and the HIF1α-KD#3 cell lines under normoxic (N) and hypoxic (H, 24 h 1% O_2) conditions. The hypoxia-induced fold change in the mRNA expression level is shown. Data are presented as mean±s.d., $n\geq6$. (D) Control and HIF1α-KD MDCK cysts were grown in 3D under normoxic or hypoxic (1% O_2) conditions. At day 6 the cysts were fixed and stained for the apical membrane marker podocalyxin (green), actin (phalloidin, red) and nuclei (DAPI; blue). A single confocal slice from the middle of the cysts is shown. Scale bars: 20 µm. (E) Quantification of the cyst phenotypes in control and HIF1α-KD MDCK cell lines grown as in D. The percentage of cysts with a single lumen were calculated and averaged from 4–8 independent experiments. A minimum of 160 cysts per sample was scored in each experiment. Data are presented as mean±s.d., $n\geq4$. *P<0.05; **P<0.001; ***P<0.0001; ns, not significant (Student's t-test for pairwise comparisons).

Journal of Cell Science

Journal of Cell Science (2018) 131, jcs210906. doi:10.1242/jcs.210906

performed using HIF1α-KD clone #3, which had the highest (95% at mRNA level) silencing. Similar data were obtained with the other two clones, with the penetrance of the phenotype correlating with the knockdown efficiency (as shown for clone #1 in Fig. 1E). MDCK cells infected with a retrovirus containing an empty short hairpin RNA (shRNA) expression cassette were used as a control in all experiments.

To examine the hypoxia response in WT and HIF1α-KD MDCK cells, we performed a qRT-PCR analysis of selected known HIF target genes. Whereas the WT cells responded to hypoxia (1% O_2, 24 h) by upregulation of the mRNA levels of adrenomedullin (*ADM*), aldolase C fructose-bisphosphate (*ALDOC*), BCL2/adenovirus E1B (*BNIP3*), BCL2/adenovirus E1B 19 kDa interacting protein 3-like (*BNIP3L*), vascular endothelial growth factor A (*VEGFA*) and lysyl oxidase (*LOX*), HIF1α-KD cells failed to efficiently induce these target genes (Fig. 1C). It should be noted that the extent of hypoxic induction of a particular gene depends on the cell type and experimental conditions; the range in the case of the MDCK cells in our experimental setup being from ∼2-fold (LOX) to ∼20-fold (ADM) induction. Irrespective of the magnitude of the hypoxic induction, knockdown of HIF1α reduced it in a statistically significant manner.

Next, we studied the effects of hypoxia on epithelial morphogenesis by culturing the WT and HIF1α-KD MDCK cells in 3D basement membrane extract (BME) gels, where they form hollow cysts lined by one layer of polarized cells under normal conditions (Myllymäki et al., 2011). All cultures were initially grown in normoxic conditions for 1 h, after which half of the cultures were transferred to hypoxia (1% O_2) and cultured for 6 days. During normoxia, ∼80% of the WT MDCK cells formed hollow spherical cysts with the apical surface of the epithelial cells lining the lumen (hereafter denoted as the regular cyst phenotype) as determined by podocalyxin staining (Fig. 1D,E). The apical membrane also stained strongly with phalloidin, indicating formation of actin-rich microvilli (Fig. 1D). In contrast, under hypoxic conditions most of the WT MDCK cysts lacked a central organized lumen, displayed an irregular podocalyxin staining pattern and the most intense actin staining at the basal surface facing the BME gel (Fig. 1D,E). Interestingly, the vast majority of the HIF1α-KD cysts were of regular phenotype in both normoxic (76.5%) and hypoxic (74%) conditions (Fig. 1D,E).

HIF1α modulates EMT and TGFβ signaling pathways under hypoxic conditions

To screen for potential signaling pathways involved in the hypoxia-induced morphogenetic changes in wild-type MDCK cells in 3D BME gels (Fig. 1D), we performed microarray-based gene expression analysis in WT and HIF1α-KD MDCK cells grown under normoxic and hypoxic conditions for 6 days. The microarray analysis suggested that there were changes in the expression of a number of genes associated with EMT and TGFβ signaling pathways between the WT and HIF1α-KD MDCK cells during hypoxia (results deposited in the Gene Expression Omnibus database under accession number GSE94772).

EMT is regulated by a complex network of transcription factors, such as the Snail family zinc finger 1 and 2 (SNAI1 and SNAI2) and the zinc finger E-box-binding homeobox 1 (ZEB1) (Kalluri and Weinberg, 2009). Downregulation of E-cadherin and upregulation of vimentin are two well-documented indications of EMT, and the expression levels of these proteins can be regulated at both transcriptional and post-translational level (Kalluri and Weinberg, 2009). Culture of the MDCK cells in hypoxic conditions led to a ∼2–3-fold induction of the *SNAI1* and *SNAI2* mRNAs, whereas no hypoxia-inducibility of *ZEB1*, E-cadherin and vimentin mRNAs was observed (Fig. 2A). No systematic effect of the HIF1α-KD on the mRNA expression of these EMT markers was observed during hypoxia (Fig. 2A). Expression of E-cadherin protein (Fig. 2B,C) was in line with the observed mRNA levels (Fig. 2A). The relative amount of vimentin protein was increased by ∼5-fold in hypoxic versus normoxic conditions in WT cells, while in HIF1α-KD cells, this hypoxic induction was significantly reduced (Fig. 2C,D). Despite these observed effects and the abnormal cystogenesis in hypoxic MDCK cells (Fig. 1C,D), the tight junction marker ZO-1 displayed restricted subapical localization around small lumens in multilumenal hypoxic MDCK cysts, which remained as tight epithelial clusters and did not display invasive mesenchymal morphology (Fig. S1A).

EMT is a multistep process where TGFβ signaling is known to regulate the transition between epithelial and mesenchymal state (Kalluri and Weinberg, 2009). During hypoxia, the mRNA expression levels of the studied TGFβ ligands, receptors and effectors were systematically downregulated in HIF1α-KD cells when compared with WT cells, with the exception of TGFβ3 and TGFβR2 (Fig. 2E). In line with this, microarray analysis showed downregulation of multiple TGFβ target genes, such as for example *CDKN1A*, *COL1A1*, *COL1A2*, *COL3A1* and *IGF1* in the HIF1α-KD cells. However, PAI1 (also known as SERPINE1), a commonly used marker for TGFβ pathway activation was significantly upregulated in hypoxic HIF1α-KD cells according to the microarray analysis. It should be noted that PAI1 is a well-known HIF2 target (Geis et al., 2015; Meade et al., 2007; Suzuki et al., 2014), which is likely to explain this effect. qRT-PCR analysis shown for *CDKN1A*, *CDC25A* and *PAI1* (Fig. 2E) was in line with the microarray data analysis. Given that it is common that there are post-translational regulatory mechanisms for growth factor receptors, we also analyzed the TGFβR1 and TGFβR2 protein levels. Both of these receptors were downregulated at protein level in hypoxic HIF1α-KD cells (Fig. 2G–J). TGFβR1 colocalized with the tight junction protein marker zonula occludens 1 (ZO-1) in both 2D and 3D MDCK cultures, and HIF1α-KD or hypoxia did not affect the localization (Fig. S2A,B). These data suggest that HIF1α-KD affects the TGFβ signaling cascade.

TGFβ signaling is required for hypoxia-induced loss of cyst polarization

Given the observed HIF1α-dependent modulation of the TGFβ pathway, we next wanted to address whether activation of TGFβ signaling mediates the hypoxia-induced perturbation of cyst formation. To this end, WT and HIF1α-KD cells were seeded into 3D BME gels and subjected to normoxic or hypoxic conditions in the presence of SB431542, an inhibitor of TGFβR1, or in the presence of recombinant active TGFβ1 (Fig. 3A,B). Addition of SB431542 to WT MDCK cell cultures did not interfere with cyst polarization during normoxia but partially rescued central lumen formation under hypoxic conditions, while SB431542 did not affect cystogenesis of the HIF1α-KD cells (Fig. 3A,B). Upon addition of recombinant active TGFβ1, cystogenesis was severely disturbed in both WT and HIF1α-KD MDCK cells during normoxia and hypoxia (Fig. 3A,B). These functional data suggest that hypoxia-mediated stabilization of HIF1α disrupts polarized morphogenesis in a TGFβ-signaling-dependent manner. Because addition of active TGFβ bypasses HIF1α-KD induced effects on polarity, it seems likely that HIF1α regulates an early step in hypoxia-driven TGFβ activation, possibly expression or activation of the latent TGFβ and TGFβR complexes.

Smads are central players in the TGFβ signaling pathway, operating downstream of the TGFβR engagement (Massagué and

Journal of Cell Science (2018) 131, jcs210906. doi:10.1242/jcs.210906

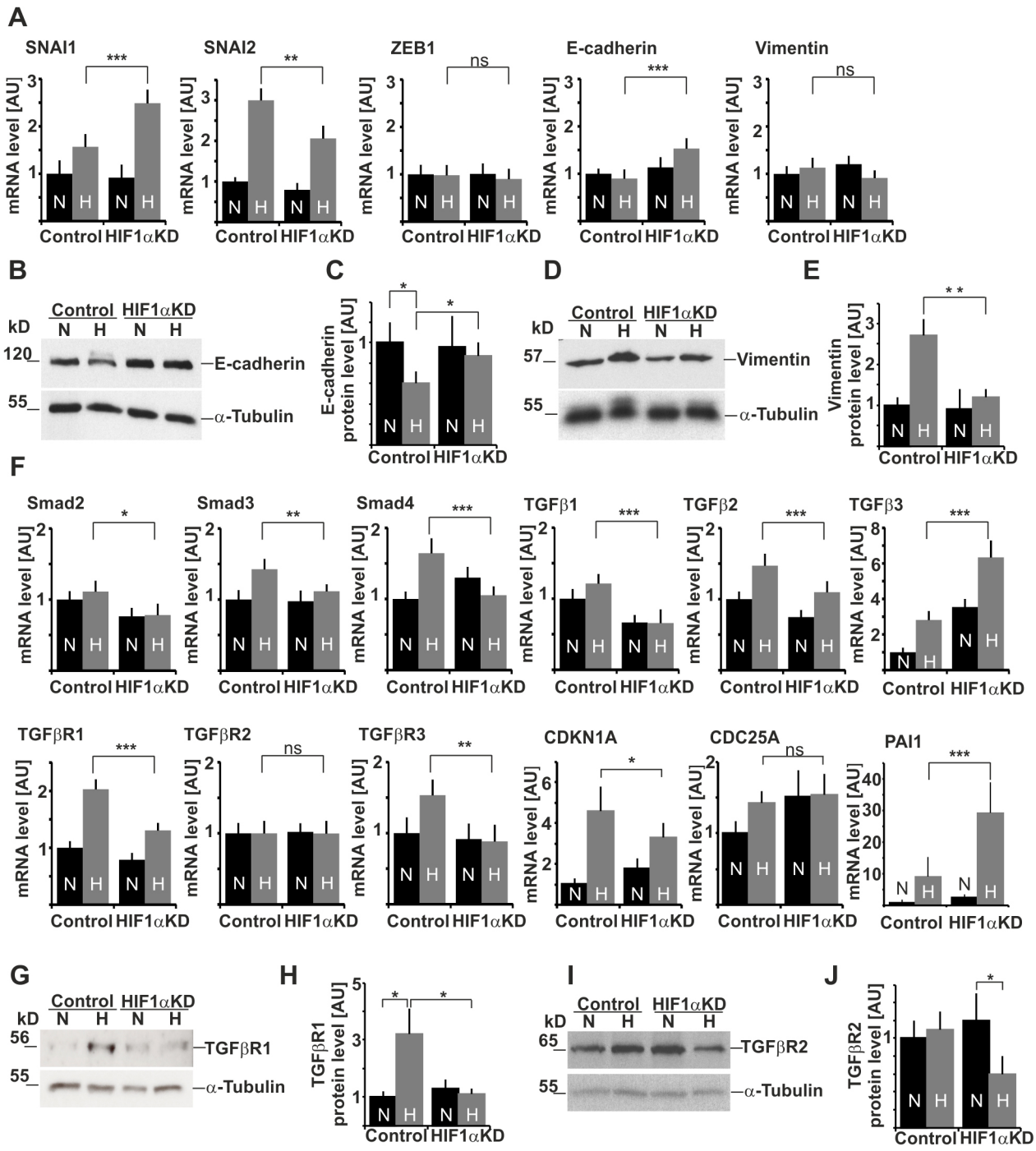

Fig. 2. Expression of genes involved in EMT and TGFβ pathways are deregulated in hypoxia. qRT-PCR analysis of the expression of mRNA encoding (A) SNAI1, SNAI2, ZEB1, E-cadherin and Vimentin, and (F) Smad2, Smad3, Smad4, TGFβ1, TGFβ2, TGFβ3, TGFβR1, TGFβR2, TGFβR3, CDKN1A, CDC25A and PAI1 in control and HIF1α-KD#3 cell lines cultured in 2D in normoxic (N) and hypoxic (H, 24 h 1% O_2) conditions. Data are presented as mean±s.d., $n \geq 4$, of relative expression levels with respect to those in normoxic control cells. (B–J) Western blot analysis of (B) E-cadherin, (D) Vimentin, (G) TGFβR1 and (I) TGFβR2 in control and HIF1α-KD#3 cell lines cultured in 2D in normoxic (N) and hypoxic (H, 24 h 1% O_2) conditions. α-tubulin is shown as a loading control. Quantifications of western blot data of (C) E-cadherin, (E) vimentin, (H) TGFβR1 and (J) TGFβR2 protein levels. Data are presented as mean±s.d. (n=4) of relative expression levels with respect to those in normoxic controls. *P<0.05; **P<0.001; ***P<0.0001; ns, not significant (Student's t-test for pairwise comparisons). AU, arbitrary units.

Gomis, 2006). In order to confirm the involvement of TGFβ pathway in the disruption of hypoxic cystogenesis, we studied the kinetics of Smad2 phosphorylation in WT and HIF1α-KD MDCK cells upon exposure to hypoxic conditions for different time periods (Fig. 3C,D). The total Smad2 protein level remained constant in WT cells during the 24 h incubation in hypoxic conditions, whereas phosphorylation of Smad2 (pSmad2) increased strongly, peaking at 18 h (Fig. 3C,D). In contrast, HIF1α-KD abolished such a peak in Smad2 phosphorylation during hypoxia (Fig. 3C,D,F).

Journal of Cell Science

Journal of Cell Science (2018) 131, jcs210906. doi:10.1242/jcs.210906

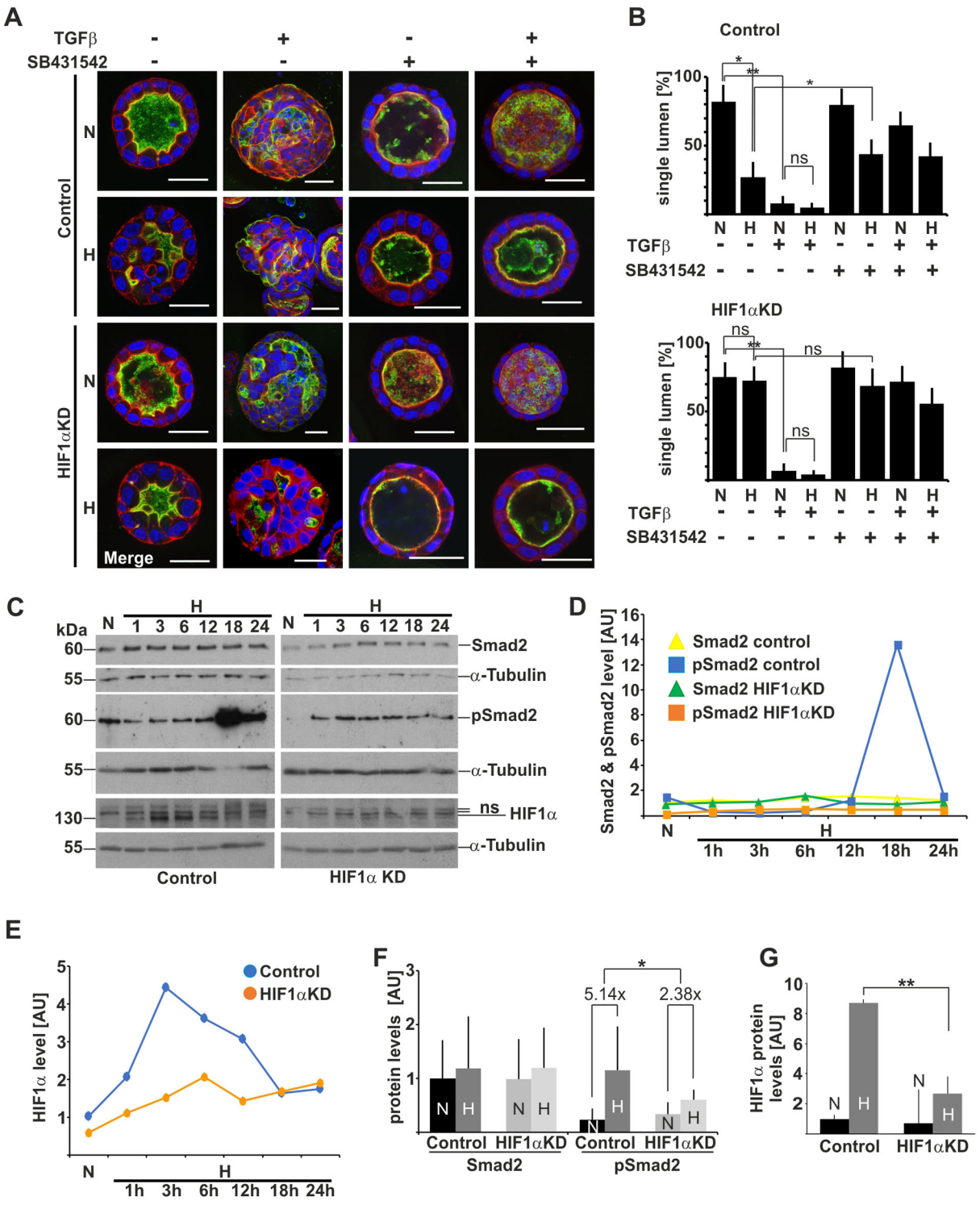

Fig. 3. Activated TGFβ signaling disrupts cyst polarization during hypoxia. (A) Control and HIF1α-KD MDCK cysts were grown in 3D BME gels under normoxic (N) or hypoxic (H, 1% O_2) conditions with and without recombinant human TGFβ, and with and without inhibitor SB431542 being added, as indicated (on the second and fourth days of culture). At day 6 the cysts were fixed and stained for an apical membrane marker podocalyxin (green), actin (red) and nuclei (DAPI, blue). A single confocal slice from the middle of the cysts is shown. Scale bars: 20 µm. (B) Quantification of the cyst phenotypes in control and HIF1α-KD MDCK cells grown as in A. The percentage of cysts with a single lumen was calculated and averaged from 4–6 independent experiments. A minimum of 160 cysts per sample was scored in each experiment. Data is presented as mean±s.d. (n=3). (C) Western blot analysis of Smad2, pSmad2 and HIF1α protein levels in control and HIF1α-KD cells cultured in 2D under normoxic (N) or hypoxic (H, 1% O_2) conditions for 1, 3, 6, 12, 18 and 24 h. α-tubulin is shown as a loading control. Quantification of this blot is shown in (D) for Smad2 and pSmad2, and in (E) for HIF1α protein. (F,G) Control and MDCK cells were cultured in 2D under normoxic (N) or hypoxic (H) conditions for 18 h followed by lysis and western blot analysis of (F) Smad2 and pSmad2 levels or (G) HIF1α protein levels. For Smad2 and pSmad2 quantification, the data are presented as mean±s.d. (n=3) of relative expression with respect to Smad2 expression in normoxic control cells, and for HIF1α quantification, data is presented as mean±s.d. (n=3) relative to HIF1α expression in normoxic control cells. *P<0.05; **P<0.001; ns, not significant (Student's t-test for pairwise comparisons). AU, arbitrary units.

Journal of Cell Science (2018) 131, jcs210906. doi:10.1242/jcs.210906

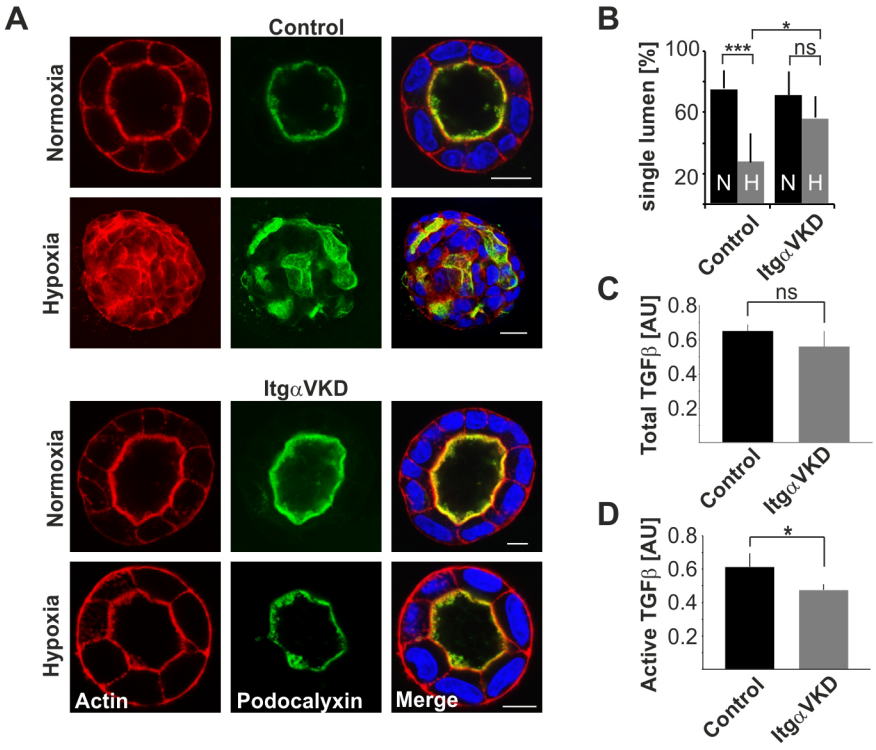

Fig. 4. Knockdown of ItgαV rescues cyst polarization in hypoxia. (A) Control and ItgαV-KD MDCK cysts were grown in 3D BME gels under normoxic or hypoxic (1% O_2) conditions. At day 6, the cysts were fixed and stained for the apical membrane marker podocalyxin (green), actin (red) and nuclei (DAPI, blue). A single confocal slice from the middle of the cysts is shown. Scale bars: 20 µm. (B) Quantification of the cyst phenotypes in control and ItgαV-KD MDCK cell lines grown as in A. N, normoxic conditions; H, hypoxic conditions. The percentage of cysts with a single lumen (black), or with a poorly formed or no lumen (white) was calculated and averaged from 4–8 independent experiments. Data is presented as mean±s.d. (n=3). A minimum of 160 cysts per sample was scored in each experiment. (C) Total and (D) active TGFβ-levels were measured from conditioned medium from control and ItgαV-KD MDCK cells cultured in 2D in normoxia. Data is presented as mean±s.d. (n=3). *P<0.05; ***P<0.0001; ns, not significant (Student's t-test for pairwise comparisons). AU, arbitrary units.

TGFβ is secreted as a large latent complex and must be activated before it can bind to the TGFβR complex to trigger signaling. Given the known role of αV integrins in the activation of latent TGFβ (Arjaans et al., 2012), we studied whether αV integrin (ItgαV) function is necessary for the hypoxia-induced loss of polarity. We cultured ItgαV-KD MDCK cells (Teräväinen et al., 2013) for 6 days in 3D BME gels under normoxic and hypoxic conditions. Depletion of αV integrin did not disturb cystogenesis during normoxia, as ∼75% of the WT MDCK cells and ∼72% of the ItgαV-KD MDCK cells formed polarized cysts with a hollow lumen during the 6 day culture in normoxic conditions (Fig. 4A,B). Remarkably, while the majority (73%) of WT cells failed to form polarized cysts with a lumen during hypoxia, more than half (56%) of ItgαV-KD cysts displayed polarized central lumens under these conditions (Fig. 4A,B). Moreover, a tendency towards lower levels of total secreted TGFβ and a statistically significant reduction in the levels of active TGFβ was observed in ItgαV-KD cells when compared to WT cells (Fig. 4C,D). This data shows that αV integrins are required for the hypoxia-induced loss of polarity, presumably because of their important role in the activation of latent TGFβ.

We next measured the amount of total and active TGFβ1 in the culture medium of hypoxic WT and HIF1α-KD MDCK cells. The HIF1α-KD cells displayed a significantly lower amount of both total and active secreted TGFβ relative to WT cells (Fig. 5A). Furthermore, we analyzed the mRNA and protein levels of latent TGFβ-binding protein 1 (LTBP1) and the data showed that both the

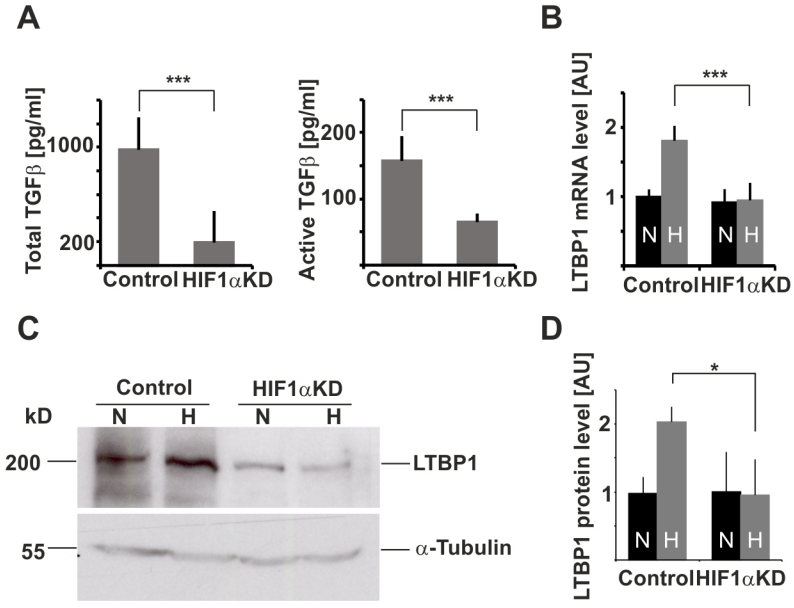

Fig. 5. Knockdown of HIF1α decreases secretion and activation of TGFβ. (A) The total (latent and active) and active TGFβ1 amount in conditioned medium from of control and HIF1α-KD MDCK cell lines cultured in hypoxia (24 h 1% O_2) in 2D. Data are presented as mean±s.d., n=3. (B) qRT-PCR and (C,D) Western blot analysis of LTBP1 mRNA and protein expression levels in control and HIF1α KD#3 cell lines cultured in 2D in normoxia (N) and hypoxia (H, 6 days 1% O_2). Data in B is presented as mean±s.d. (n=3) of relative expression levels with respect to those in normoxic control cells; data in D is presented as mean±s.d. (n=3) of protein expression levels in normoxia and hypoxia, α-tubulin was used as a loading control. *P<0.05; **P<0.001; ***P<0.0001; ns, not significant (Student's t-test for pairwise comparisons). AU, arbitrary units.

Journal of Cell Science (2018) 131, jcs210906. doi:10.1242/jcs.210906

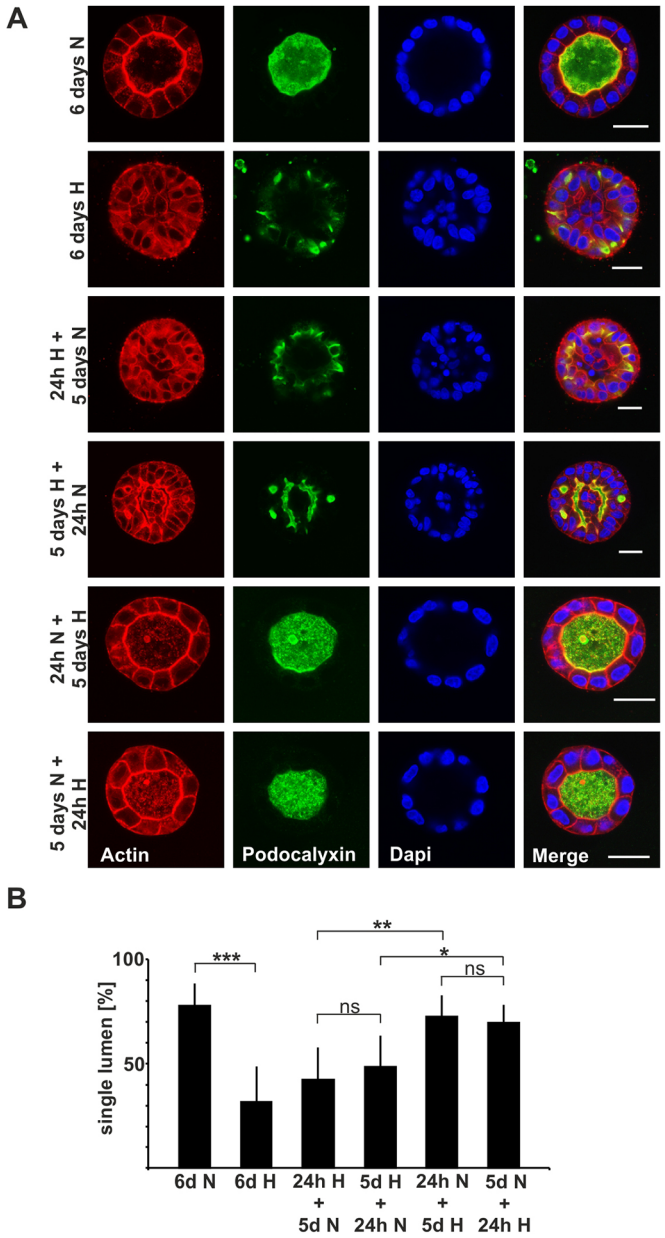

Fig. 6. Polarized cysts are resistant to hypoxia-induced morphological changes. (A) Control and HIF1α-KD MDCK cysts were grown in 3D BME gels under normoxic (N) or hypoxic (H, 1% O_2) conditions using different time regimes as indicated on the left of the panels. At day 6, the cysts were fixed and stained for the apical membrane marker podocalyxin (green), actin (red) and nuclei (DAPI, blue). A single confocal slice from the middle of the cysts is shown. Scale bars: 20 µm. (B) Quantification of the cyst phenotypes in control and HIF1α-KD MDCK cell lines grown as in A. The percentage of cysts with a single lumen were calculated and averaged from eight independent experiments. A minimum of 160 cysts per sample was scored in each experiment. Data are presented as mean±s.d., $n \geq 4$. *P<0.05; **P<0.001; ***P<0.0001; ns, not significant (Student's t-test for pairwise comparisons).

mRNA and protein level of LTBP1 was downregulated in HIF1α-KD MDCK cells under hypoxic conditions when compared with WT cells (Fig. 5B–D).

Taken together, the above data shows that the hypoxia-mediated stabilization of HIF1α is required for efficient activation of TGFβ signaling, which in turn leads to disruption of the polarized lumen formation in MDCK cells. Moreover, HIF1α is likely to operate upstream of TGFβR activation, because addition of recombinant active TGFβ1 readily disrupts cystogenesis during normoxia and hypoxia irrespective of the HIF1α status (Fig. 3A,B).

Polarized cysts are resistant to hypoxia-induced morphological changes

It has been reported that most of the critical events of lumen formation in 3D BME gel-embedded MDCK cells occur during the first 24 h when individual cells divide and form small cell clusters (Bryant et al., 2010). Upon initial polarization, the polarized organization of cysts with an enclosed central lumen is maintained by continuous subapical tight junctions, which seal the lumen from the basolateral side, and via precisely oriented cell divisions. In our experiments, when MDCK cells were transferred to hypoxic conditions, stabilization of HIF1α protein was observed 3–12 h after the transfer (Fig. 3C,E,G) and, based on Smad2 phosphorylation, the TGFβ pathway was activated maximally 18–24 h after (Fig. 3C,D,F). To study what is the critical timeframe when hypoxia affects the polarization, we cultured WT MDCK cells in normoxic conditions for 24 h or 5 days after which they were exposed to hypoxia for 5 days and 24 h, respectively, and vice versa, with the cultures being started in hypoxic conditions. The number of cysts with polarized central lumens, ∼70%, formed by cells that were first cultured in normoxic conditions for 24 h or 5 days followed by hypoxia, was only slightly lower than in the cells cultured continuously in normoxic conditions for 6 days (78%) (Fig. 6). In the opposite setup, when the cells were exposed to hypoxia for the first 24 h or 5 days followed by normoxia, ∼40–50% of the cysts had normal lumens, being slightly higher than in the cells cultured continuously in hypoxic conditions for 6 days (32%) (Fig. 6). These data indicate that the oxygenation status is critical for the establishment of polarity within the first 24 h, while polarized cysts are quite resistant to hypoxia-induced morphological changes. Interestingly, our data also indicate that the cellular effects caused by exposure to hypoxia during the early stage of cystogenesis when cells are still non-polarized, are maintained (for a prolonged time) even after the cells have been returned to normoxic conditions.

Inactivation of BAMBI restores polarized morphogenesis during hypoxia

In order to characterize the key HIF1α target genes regulating TGFβ signaling, we looked into the microarray data for the most efficiently downregulated hypoxia-responsive genes in the HIF1α-depleted cells. One such candidate gene was BMP and activin membrane-bound inhibitor (*BAMBI*), which has been previously implicated in the regulation of BMP/activin/TGFβ signaling (Onichtchouk et al., 1999; Tsang et al., 2000). BAMBI is structurally related to the type I receptors of the TGFβ family, but it lacks a functional serine/threonine kinase domain and is generally thought to function as an inhibitory pseudoreceptor for TGFβ/BMP signaling pathways, but opposing effects have also been reported (Gonzales et al., 2010; Massagué et al., 2005; Sasaki et al., 2004; Zhang et al., 2016). qRT-PCR analysis confirmed hypoxia-dependent upregulation of *BAMBI* mRNA in WT but not in HIF1α-KD MDCK cells (Fig. 7A). The *BAMBI* mRNA expression level was also robustly downregulated in normoxic HIF1α-KD relative to WT cells (Fig. 7A). This is not unexpected, as accumulating evidence indicates that HIF1 has important roles even during normoxia although being present at a low level (Bárdos and Ashcroft, 2005; Sakamoto et al., 2014). To study the functional role of BAMBI in MDCK cells, we designed two guide RNA (gRNA) constructs targeting canine BAMBI (Table S2) and

Journal of Cell Science (2018) 131, jcs210906. doi:10.1242/jcs.210906

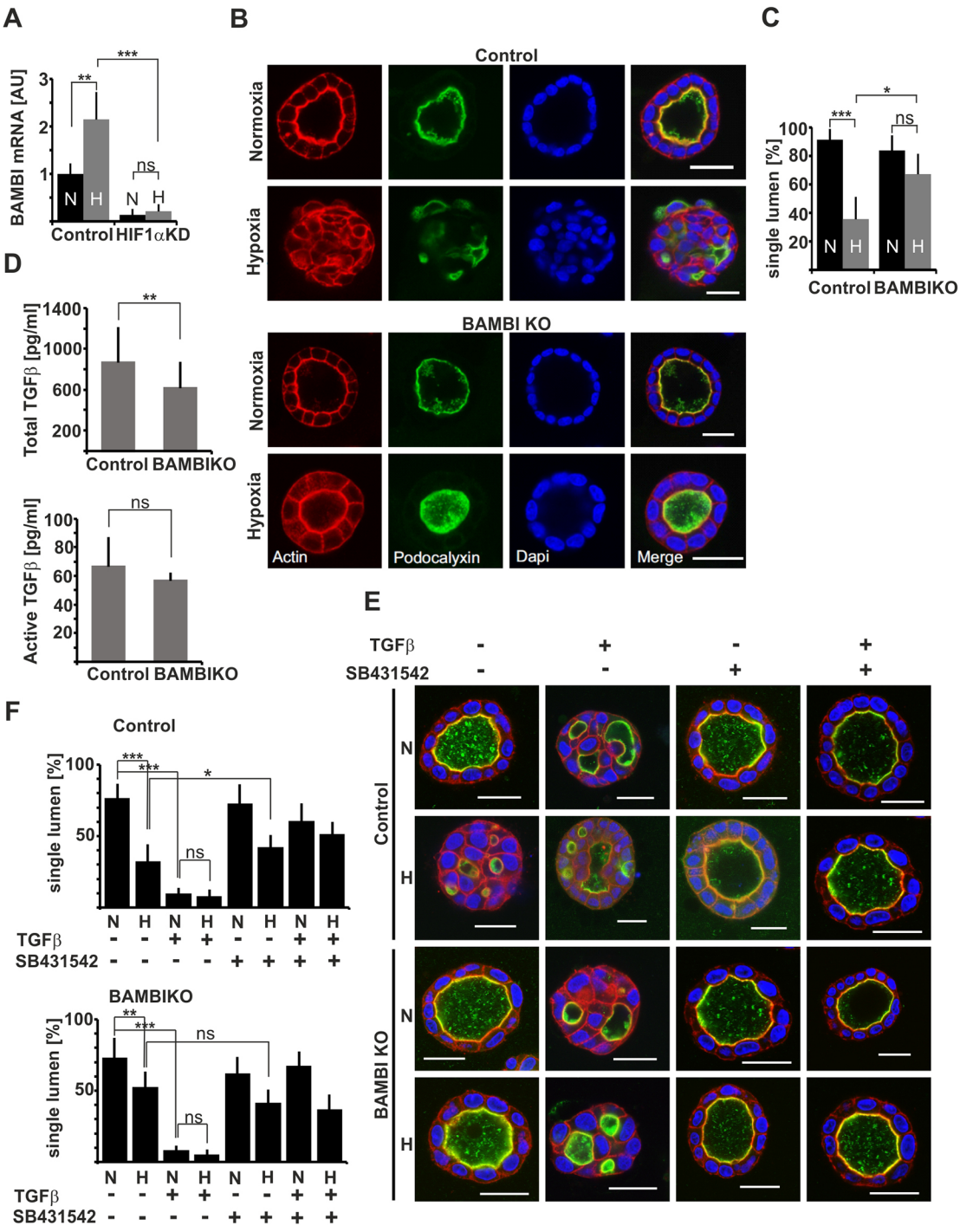

Fig. 7. Knockout of BAMBI rescues cyst polarization in hypoxia. (A) qRT-PCR analysis of *BAMBI* mRNA expression in control and HIF1α-KD#3 cell lines cultured in 2D in normoxic (N) and hypoxic (H, 24 h 1% O_2) conditions. Data are presented as mean±s.d., *n*=3. (B) Control and BAMBI-KO MDCK cysts were grown in 3D BME gels under normoxic or hypoxic (1% O_2) conditions. At day 6, the cysts were fixed and stained for the apical membrane marker podocalyxin (green), actin (red) and nuclei (DAPI, blue). A single confocal slice from the middle of the cysts is shown. Scale bars: 20 µm. (C) Quantification of the cyst phenotypes in control and BAMBI-KO MDCK cell lines grown as in B. The percentage of cysts with single lumen was calculated and averaged from three independent experiments for each of the two subclonal cell lines. A minimum of 160 cysts per sample was scored in each experiment. Data are presented as mean±s.d., *n*=6 (three independent analyses of the two subclonal cell lines). (D) Total (latent and active) and active TGFβ1 amount in conditioned media of control and BAMBI-KO MDCK cell lines cultured in 2D in hypoxia (24 h 1% O_2). Data are presented as mean±s.d., *n*=6 (three independent analyses of the two subclonal cell lines), ****P*<0.0001 (Student's *t*-test for pairwise comparison). (E) Control and BAMBI-KO MDCK cysts were grown in 3D BME gels under normoxic (N) or hypoxic (H, 1% O_2) conditions with and without recombinant human TGFβ, and with and without inhibitor SB431542 being added, as indicated (on the second and fourth days of culture). At day 6, the cysts were fixed and stained for the apical membrane marker podocalyxin (green), actin (red) and nuclei (DAPI, blue). A single confocal slice from the middle of the cysts is shown. Scale bars: 20 µm. (F) Quantification of the control and BAMBI-KO cyst phenotypes grown as in A. The percentage of cysts with single lumen was calculated and averaged from three independent experiments for each of the two subclonal cell lines. A minimum of 160 cysts per sample was scored in each experiment. Data are presented as mean±s.d. **P*<0.05; ***P*<0.001; ****P*<0.0001; ns, not significant (Student's *t*-test for pairwise comparisons). AU, arbitrary units.

Journal of Cell Science (2018) 131, jcs210906. doi:10.1242/jcs.210906

generated two independent BAMBI-KO clones (Table S3) by using the lentiCRISPR methodology (Ran et al., 2013). Successful editing of both alleles in the first exon leading to premature stop codon was confirmed by sequencing (Table S3). MDCK cells infected with non-targeting lentiCRISPR virus were used as a control in all experiments. Control and BAMBI-KO MDCK cells were seeded into 3D BME gels and grown in normoxic and hypoxic conditions. During normoxia, the control cells efficiently formed hollow cysts with a polarized lumen (91%), while, during hypoxia, a polarized central lumen was formed in only 36% of the cysts (Fig. 7B,C). Interestingly, the majority of BAMBI-KO MDCK cells formed polarized cysts under both normoxia (84%) and hypoxia (67%) (Fig. 7B,C).

HIF1-dependent activation of TGFβ signaling was herein found to be essential for hypoxia-induced disruption of cystogenesis

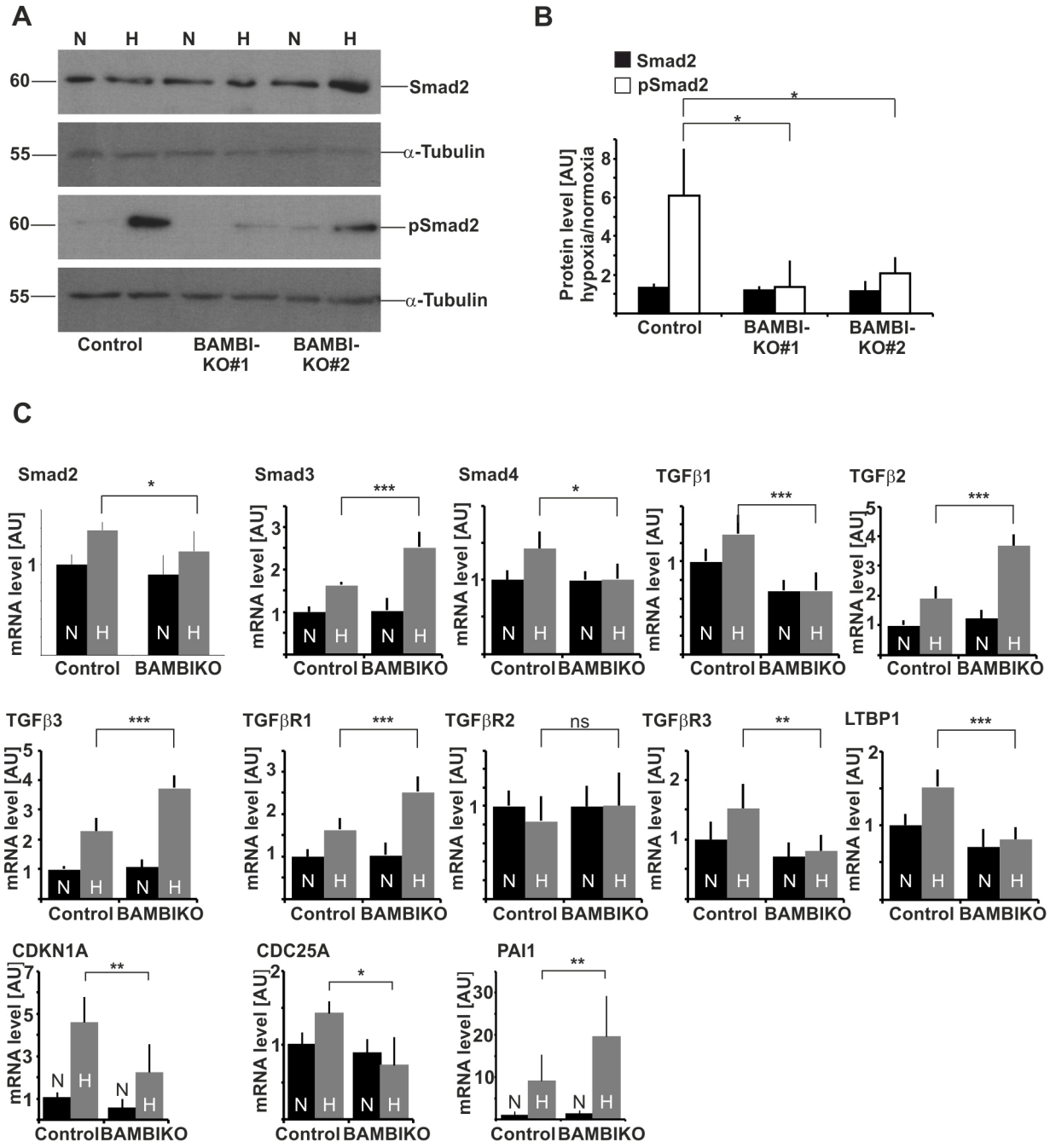

Fig. 8. BAMBI expression is required for hypoxia-induced activation of TGFβ signaling in MDCK cells. (A) Western blot analysis of Smad2 and pSmad2 in control and in BAMBI-KO cells cultured in 2D in normoxic conditions (N) or in hypoxic (H) conditions for 24 h. α-tubulin is shown as a loading control. (B) Quantification of Smad2 and pSmad2 protein levels. Data is presented as mean±s.d., n=8 (four independent experiments for each of the two subclonal cell lines), of the ratio of protein expression level in hypoxia relative to normoxia. (C) qRT-PCR analysis of mRNA expression levels of TGFβ signaling-related genes (encoding Smad2, Smad3, Smad4, TGFβ1, TGFβ2, TGFβ3, TGFβR1, TGFβR2, TGFβR3, LTBP1, CDKN1A, CDC25A and PAI1) in control and BAMBI-KO cells in 2D in normoxic and hypoxic (24 h, 1% O_2) conditions. Data are presented as mean±s.d., $n\geq6$ (at least three independent experiments for each of the two subclonal cell lines), of relative expression levels with respect to those in normoxic control cells. *P<0.05; **P<0.001; ***P<0.0001; ns, not significant (Student's t-test for pairwise comparisons). AU, arbitrary units.

Journal of Cell Science

Journal of Cell Science (2018) 131, jcs210906. doi:10.1242/jcs.210906

(Fig. 3). To see whether BAMBI operates on this same pathway, we first measured the amount of total and active TGFβ1 in the culture medium of hypoxic WT and BAMBI-KO MDCK cells. The BAMBI-KO cells displayed a significantly lower amount of total secreted TGFβ and a tendency (although not statistically significant) to a reduced amount of activated TGFβ in comparison to WT (Fig. 7D). Next, we cultured WT and BAMBI-KO cells in 3D and treated them with recombinant TGFβ and/or TGFβR1 inhibitor (SB431542). Similar to what was found in HIF1α-KD cells, addition of TGFβ1 into BAMBI-KO cultures had perturbed cystogenesis both under normoxic and hypoxic conditions, whereas treatment with SB431542 led to modest improvement in the polarization of WT, but not of BAMBI-KO, cysts during hypoxia (Fig. 7E,F). Importantly, Smad2 phosphorylation was clearly inhibited in BAMBI-KO cells indicating that, in addition to HIF1α, expression of BAMBI is required for hypoxia-induced activation of TGFβ signaling in MDCK cells (Fig. 8A,B). qRT-PCR analysis of the key genes in the TGFβ pathway revealed that BAMBI expression significantly contributed to hypoxia-driven induction of genes encoding TGFβ1, Smad2, Smad4, TGFβR3, LTBP1, CDKN1A and CDC25A (Fig. 8C). Similar to HIF1α-KD MDCK cells (Fig. 2E), BAMBI-KO MDCK cells had an elevated expression level of PAI1 during hypoxia (Fig. 8C).

DISCUSSION

In the present work, we show that hypoxia interferes with epithelial apical-basal polarization by promoting activation of the TGFβ pathway in a HIF1α-dependent manner. We identified BAMBI as a novel HIF-regulated gene that was required for hypoxia-induced activation of TGFβ signaling leading to loss of cyst polarity. TGFβ pathway is a well-known regulator of EMT in several epithelial cell types and hypoxia is also known to contribute to EMT. Hypoxia appears to enhance TGFβ-driven signaling although the mechanistic details are somewhat unclear. Hypoxia upregulates Smad3 expression and HIF1α has been shown to interact with the HIF-responsive elements (HREs) located in the TGFβ1 and TGFβ3 promoter regions (Breitkopf et al., 2006; Hung et al., 2013; Sánchez-Elsner et al., 2001; Schäffer et al., 2003). Here, we found that HIF1α depletion suppressed hypoxia-induced upregulation of Smad3 and several TGFβ pathway-related genes. In line with these findings, HIF1α-KD MDCK cells also secreted less TGFβ, produced reduced levels of LTBP1 and failed to induce Smad2 phosphorylation upon exposure to hypoxia.

Importantly, we demonstrate that the hypoxia-induced loss of polarity was dependent on TGFβ signaling downstream of HIF1α function. Whereas HIF1α expression peaked 3 h after exposure to hypoxia, robust Smad2 phosphorylation was observed much later, at 18 h post hypoxia. TGFβ is secreted from cells as a large latent complex that associates with extracellular matrix, and can be mechanically activated by integrins, αV integrins being particularly important in this process (Annes et al., 2004; Wipff and Hinz, 2008). In line with this, inhibition of αV integrin expression also prevented HIF1α-mediated effects on epithelial polarity.

EMT-associated phenotypic changes can be facilitated by many different pathways. Notch signaling has been proposed to synergize with the TGFβ- and hypoxia-response pathways to induce EMT, and HIF1α has been shown to directly interact with the intracellular domain of Notch (Gonzalez and Medici, 2014; Jiang et al., 2011; Poellinger and Lendahl, 2008). Notch directly upregulates SNAI1 and has been shown to be required for hypoxia-induced upregulation of SNAI1 and SNAI2 (Chen et al., 2010; Sahlgren et al., 2008). However, while hypoxia-induced *SNAI2* expression was slightly less prominent in HIF1α-KD MDCK cells in our experiments, the expression level of *SNAI1* mRNA was even higher in hypoxic HIF1α-KD cells when compared to control cells. Therefore, further studies are needed to clarify whether Notch signaling contributes to disruption of polarity in HIF1α-KD cells.

We identified BAMBI as a hypoxia-inducible gene that was drastically downregulated in HIF1α-KD MDCK cells, and its inactivation rescued epithelial cell polarization during hypoxia. BAMBI is a transmembrane protein that structurally resembles the TGFβR1 and BMPR1 (Onichtchouk et al., 1999). However, it lacks the cytoplasmic kinase domain and is therefore generally thought to function as a negative regulator of both TGFβ and BMP signaling (Guillot et al., 2012; Tsang et al., 2000). In line with this, depletion of BAMBI expression reportedly enhances the TGFβ signaling response in cancer cell lines (He et al., 2016; Marwitz et al., 2016). Contrary data have also been reported, however, as high levels of BAMBI expression have been correlated with increased plasma TGF-β1 levels in chronic obstructive pulmonary disease patients (Zhang et al., 2016). Here, we found that BAMBI expression was strongly downregulated in HIF1α-depleted cells in which TGFβ signaling was inhibited. Bioinformatic analysis identified 24 putative HREs near the promoter region of the canine *BAMBI* gene, two of which are conserved in the human *BAMBI* gene (data not shown). Depletion of BAMBI expression restored polarization in hypoxic conditions, and BAMBI was found to contribute to the activation of the TGFβ pathway in hypoxic MDCK cells. Similar to HIF1α-KD cells, BAMBI-KO cells modulated the expression of some of the key genes in the TGFβ pathway and BAMBI-KO cells failed to efficiently induce Smad2 phosphorylation upon exposure to hypoxia. While many of the target genes, such as those encoding TGFβ1, LTBP1, TGFβR3, Smad2 and Smad4, were regulated in both the HIF1α-KD cells and BAMBI-KO cells, there were also differences suggesting that although BAMBI clearly regulated hypoxia-induced loss of cyst polarity, not all of the effects of HIF1α are mediated by BAMBI. BAMBI is identified here as a novel HIF1α-regulated protein that plays an important role during hypoxia-driven modulation of TGFβ signaling and thereby epithelial morphogenesis.

MATERIALS AND METHODS

Cell culture

MDCK strain II cells (ATCC:CCL-34) were used in this study. For 2D and 3D culture, cells were grown as described previously (Friedrichs et al., 2007; Myllymäki et al., 2011). MDCK cells were cultured either in normoxic or hypoxic (1% O_2, 5% CO_2 and 94% N_2) conditions in an Invivo2 400 hypoxic workstation (Baker Ruskinn, Sanford, ME). The cells were regularly tested, every 6 months, for mycoplasma contamination.

Generation of HIF1α-KD cells by retrovirus-mediated RNA interference

HIF1α-KD cell lines were generated by infection of MDCK cells with retroviruses coding for shRNA constructs, and selection of infected cells was achieved with puromycin as previously described (Myllymäki et al., 2011). Three targeting sequences were cloned into the RVH1-puro vector and their efficiencies to silence HIF1α expression in MDCK cells were determined by qRT-PCR (Table S1).

Generation of BAMBI-KO cells by lentivirus-mediated expression of sgRNAs and Cas9

Gene editing with lentivirus-mediated co-expression of Cas9 and single-guide RNA (sgRNA) constructs was performed as previously described

(Shalem et al., 2014) with some modifications. The first exon of the canine *BAMBI* was used as a template for gRNA design. Target sequences with no off target sites with less than three mismatches in the canine genome database (European Nucleotide Archive), were selected based on the FASTA similarity search-tool (EMBL-EBI). Two targeting sequences were selected and the corresponding gRNA oligonucleotides with BsmBI overhangs (Sigma-Aldrich, St Louis, MO) were subcloned into lentiCRISPRv1 (Table S2). Production of lentivirus and transfection were performed as described previously (Shalem et al., 2014). Puromycin-resistant cells were subcloned by fluorescence-activated cell sorting. Subclonal cell lines were generated and sequenced as described previously (Shalem et al., 2014), and two subclonal cell lines generated from the two gRNA constructs, BAMBIKO#1 and BAMBIKO#2, respectively, were used as biological replicates (Table S3).

Reagents

Recombinant human TGFβ1 (100-21, PeproTech, Stockholm, Sweden) was reconstituted in 10 mM citric acid pH 3.0, at a final stock concentration of 1 µg/ml according to the manufacturer's protocol, and stored at −20°C. SB431542 (1614, Tocris Bioscience, Bristol, UK), a selective inhibitor of TGFβR1 was stored at a concentration of 5 µM in dimethyl sulfoxide (DMSO) at −20°C.

Immunostaining

For immunostaining, 3D MDCK cells in 30 µl blobs of Cultrex® 3D Culture Matrix™ BME (3445-005-01, Trevigen, Gaithesburg, MD) were cultured in normoxic or hypoxic conditions for 6 days. For immunostaining with anti-podocalyxin antibody (3F2/D8 cell line, Developmental Studies Hybridoma Bank, Iowa City, IA), anti-E-cadherin antibody (rr1, 1:100, Developmental Studies Hybridoma Bank) and anti-ZO-1 antibody (339100, 1:200, Invitrogen, Carlsbad, CA), MDCK cells in Cultrex blobs were fixed with 4% paraformaldehyde in phosphate-buffered saline (PBS) for 20 min, followed by quenching with 200 mM glycine in PBS for 20 min, and permeabilization and blocking with 0.1% Triton X-100 and 0.5% bovine serum albumin (BSA) in PBS for 1 h. All steps were performed at room temperature (RT). For immunostaining of TGFβR1 (ab31013, 1:200, Abcam, Cambridge, UK) and ZO-1 (339100, 1:200, Invitrogen), 2D MDCK cells were fixed with ice-cold methanol for 20 min at 4°C, followed by blocking with 0.5% BSA in PBS for 1 h. Primary antibodies were added in corresponding blocking solutions and incubated overnight at 4°C. Corresponding secondary antibodies, phalloidin (ab176757, 1:2000, Abcam, Cambridge, UK), for actin staining, and DAPI (D9542, 1:500, Sigma-Aldrich), for DNA staining, were added and incubated overnight at 4°C.

Microarray analysis

2D MDCK cells were seeded at a density of 2.0×10^5 cells in 3.5-cm diameter dishes, cultured in normoxic conditions for 24 h and then transferred into hypoxic conditions for 24 h. Total RNA was isolated using an RNeasy Kit (Qiagen, Hilden, Germany) according to the manufacturer's protocol. The total RNA was reverse transcribed into cDNA by using an 3′ IVT Express Kit (Affymetrix, Santa Clara, CA), hybridized with the GeneChip Canine Genome 2.0 Array plates according to manufacturer's instructions (https://assets.thermofisher.com/TFS-Assets/LSG/manuals/expression_analysis_technical_manual.pdf) and the GeneChips were scanned with an Affymetrix gene chip scanner 3000 7G according to the manufacturer's protocol in Biocenter Oulu DNA Analysis Core Facility. Affymetrix CEL files (Gene Expression Omnibus accession number GSE94772) were normalized using pair-wise rank-invariant normalization in software dchip_2010_01.exe and analyzed using software. Changes in gene expression between the sample groups were determined using the following criteria: differentially expressed genes between WT in normoxia (A) and hypoxia (B), and HIF1α-KD MDCK cells in normoxia (C) and hypoxia (D) were identified by the comparison option of the dchip_2010_01 software. The filtering criteria for this analysis were (1) fold change D/B or B/D≥2, (2) lower confidence bound of fold change D−B or B−D=100, (3) *P* value for paired *t*-test <0.05. Differently expressed genes were analyzed by the DAVID Bioinformatics Resources.

RNA isolation and qRT-PCR

2D MDCK cells were cultured in normoxic conditions for 24 h, followed by 24 h in hypoxic or normoxic conditions. Total RNA was isolated from the 2D and 3D cells by using an RNeasy Kit (Qiagen, Hilden, Germany), according to the manufacturer's protocol. The total RNA was reverse-transcribed into cDNA using an iScript cDNA synthesis kit (Bio-Rad Laboratories, Hercules, CA). Quantitative real-time PCR (qRT-PCR) was performed using iTaq Universal SYBR Green Supermix (Bio-Rad Laboratories, Hercules, CA) and a CFX96 Touch real-time PCR detection system. Primer sequences are listed in Table S4. Expression levels were normalized to that of TATA box-binding protein.

Western blotting

2D MDCK cells were seeded at a density of 7.5×10^5 cells in 10-cm diameter dishes and cultured in normoxic conditions for 24 h and then transferred to hypoxic conditions for 3, 6, 12, 18 or 24 h. Protein was isolated using RIPA lysis buffer (25 mM Tris-HCl pH 7.8, 150 mM NaCl, 0.1% SDS, 0.5% sodium deoxycholate and 1% Triton X-100). Primary antibodies against the following proteins were used as follows: HIF1α (NB 100-479, 1:2000, Novus Biological, Littleton, CO), TGFβR1 (ab31013, 1:1000, Abcam, Abcam, Cambridge, UK), TGFβR2 (ab186838, 1:500, Abcam), Smad2 (5339S, 1:1000, Cell Signaling, Danvers, MA), pSmad2 (3108L, 1:1000, Cell Signaling), LTBP1 (sc-28132, 1:200, Santa Cruz Biotechnology, Dallas, TX), vimentin (V6630, 1:1000, Sigma-Aldrich), ZO-1 (339100, 1:500, Invitrogen), E-cadherin (rr1, 1:1000, Developmental Studies Hybridoma Bank), ItgαV (ab1930, 1:1000, Millipore, Burlington, MA) and α-tubulin (T6199, 1:20,000, Sigma-Aldrich).

Quantification of western blot data was performed from at least three independent blots. First, for every experiment, the intensities of protein bands were normalized relative to that of a loading control (α-tubulin). Secondly, normalized band intensities were adjusted relative to the average of the replicates of an appropriate sample in each experiment. For the quantification in Fig. 1A, hypoxic HIF1α levels were set to 100% and other samples are shown relative to this. In Figs 2C,E,H,J, 3G, and 5D, arbitrary proteins levels are shown relative to protein levels in normoxic control cells, which were adjusted to 1. Quantification of the hypoxia-induced Smad2 phosphorylation (Figs 3F and 8B) was achieved by first adjusting α-tubulin normalized intensities (for both Smad2 and pSmad2) relative to Smad2 value in normoxic control cells, which was set to 1. Then the value in hypoxia was divided with that found in normoxia, separately for each replicate. In all of the above cases graphs show mean±s.d. as described in each figure legend. Quantifications in Fig. 3D,E represent the value from a single blot (Fig. 3C) where α-tubulin normalized intensities for each protein are shown relative to normoxic levels in control cells, which were set to 1.

Microscopy and image acquisition

Confocal images were acquired at RT using an Olympus FluoView-1000 laser-scanning confocal microscope with an 100× UPlanSApo (NA 1.40) oil immersion objective (Olympus, Tokyo, Japan). Sequential scans were performed using 405 nm, 488 nm and 543 nm laser lines, for fluorophore excitation, coupled with DAPI (430–470 nm), GFP (505–525 nm) and Cy3 (560LP) emission filters, respectively. Images were collected with the FV10-ASW software (Olympus, Tokyo, Japan) and imported into Adobe Photoshop CS (Adobe Systems, San José, CA).

Measurement of TGFβ level

The concentration of total and active TGFβ1 in culture medium was determined by means of the TGFβ1 Emax ImmunoAssay System (G7590, Promega, Madison, WI) in Nunc immuno 96 well plates (442404, Sigma-Aldrich) according to the manufacturer's instructions with the following modifications. Cells were cultured first for 24 h in minimal essential medium (MEM; Gibco, Gaithersburg, MD) containing 5% fetal bovine serum (FBS, Thermo Fisher Scientific, Waltham, MA) after which they were washed with PBS and cultured for an additional 24 h in MEM without FBS. 100 ml samples of the culture medium were collected in sterile tubes, passed through a 0.45-µm filter to remove cell debris, concentrated to 400 µl using an Amicon Ultra-15 Centrifugal Filter Unit with Ultracel-10 membrane (UFC901024, Merck Millipore, Burlington, MA) and frozen

until analysis. To detect total TGFβ1, half of each sample was acidified with HCl to pH 3.0 for 20 min at RT and then neutralized to pH 7.6 with NaOH. Active TGFβ1 was detected in the other half of the sample according to the manufacturer's instructions. Samples were then diluted 1:2 in the provided sample buffer and incubated for 90 min at RT with shaking. The amount of latent TGFβ1 was determined as a subtraction of the active portion from the total amount of TGFβ1. Plates were read in a Multilabel Counter 1420 VICTOR3 V (Perkin Elmer, Waltham, MA) at 450 nm.

Statistical analysis

Statistical analyses for comparisons between two groups were performed using Student's two-tailed *t*-test and denoted as $*P<0.05$; $**P<0.01$; $***P<0.001$ in all experiments.

Acknowledgements

We thank R. Salmu for excellent technical assistance; H.-M. Lee for help in analysis of microarray data and the Biocenter Oulu DNA Analysis, Light Microscopy and Virus Core Facilities co-funded by the University of Oulu and Biocenter Finland for excellent technical assistance.

Competing interests

J.M. owns equity in FibroGen Inc., which develops hypoxia-inducible factor prolyl 4-hydroxylase inhibitors as potential therapeutics. The company supports research on hypoxia response signaling in the laboratory of J.M.

Author contributions

Conceptualization: A.M., J.M.; Methodology: I.R., A.M., J.M.; Validation: I.R.; Formal analysis: I.R.; Investigation: I.R., F.M., S.M.M., P.G.G., K.S.M., J.V.M.; Resources: A.M., J.M.; Writing - original draft: I.R., A.M.; Writing - review & editing: S.M.M., A.M., J.M.; Visualization: I.R.; Supervision: A.M., J.M.; Project administration: J.M.; Funding acquisition: J.M.

Funding

This work was supported Academy of Finland Research Council for Health grants [114344 (J.M.), 296498 (J.M.), 135560 (A.M.), 263770 (A.M.)] and Academy of Finland Center of Excellence 2012-2017 grant (251314 to J.M., A.M.), Sigrid Juséliuksen Säätiö (J.M.), Jane ja Aatos Erkon Säätiö (J.M.) and FibroGen Inc. (J.M.).

Data availability

Microarray data in this study has been deposited in the Gene Expression Omnibus database under accession number GSE94772.

Supplementary information

Supplementary information available online at
http://jcs.biologists.org/lookup/doi/10.1242/jcs.210906.supplemental

References

Annes, J. P., Chen, Y., Munger, J. S. and Rifkin, D. B. (2004). Integrin αVβ6-mediated activation of latent TGF-β requires the latent TGF-β binding protein-1. *J. Cell Biol.* **165**, 723-734.

Arjaans, M., Oude Munnink, T. H., Timmer-Bosscha, H., Reiss, M., Walenkamp, A. M. E., Lub-de Hooge, M. N., de Vries, E. G. E. and Schröder, C. P. (2012). Transforming growth factor (TGF)-α expression and activation mechanisms as potential targets for anti-tumor therapy and tumor imaging. *Pharmacol. Ther.* **135**, 123-132.

Bárdos, J. I. and Ashcroft, M. (2005). Negative and positive regulation of HIF-1: a complex network. *Biochim. Biophys. Acta.* **1755**, 107-120.

Breitkopf, K., Godoy, P., Ciuclan, L., Singer, M. V. and Dooley, S. (2006). TGF-β/smad signaling in the injured liver. *Z. Gastroenterol.* **44**, 57-66.

Bryant, D. M., Datta, A., Rodríguez-Fraticelli, A. E., Peränen, J., Martín-Belmonte, F. and Mostov, K. E. (2010). A molecular network for de novo generation of the apical surface and lumen. *Nat. Cell Biol.* **12**, 1035-1045.

Chen, J., Imanaka, N., Chen, J. and Griffin, J. D. (2010). Hypoxia potentiates notch signaling in breast cancer leading to decreased E-cadherin expression and increased cell migration and invasion. *Br. J. Cancer* **102**, 351-360.

Friedrichs, J., Torkko, J. M., Helenius, J., Teräväinen, T. P., Fullekrug, J., Muller, D. J., Simons, K. and Manninen, A. (2007). Contributions of galectin-3 and -9 to epithelial cell adhesion analyzed by single cell force spectroscopy. *J. Biol. Chem.* **282**, 29375-29383.

Geis, T., Döring, C., Popp, R., Grossmann, N., Fleming, I., Hansmann, M.-L., Dehne, N. and Brüne, B. (2015). HIF-2α-dependent PAI-1 induction contributes to angiogenesis in hepatocellular carcinoma. *Exp. Cell Res.* **331**, 46-57.

Gonzales, C. B., Simmons, D. and MacDougall, M. (2010). Competing roles of TGFβ and nma/BAMBI in odontoblasts. *J. Dent. Res.* **89**, 597-602.

Gonzalez, D. M. and Medici, D. (2014). Signaling mechanisms of the epithelial-mesenchymal transition. *Sci. Signal.* **7**, re8.

Guillot, N., Kollins, D., Gilbert, V., Xavier, S., Chen, J., Gentle, M., Reddy, A., Bottinger, E., Jiang, R., Rastaldi, M. P. et al. (2012). BAMBI regulates angiogenesis and endothelial homeostasis through modulation of alternative TGFβ signaling. *PLoS ONE* **7**, e39406.

He, Y., Ou, Z., Chen, X., Zu, X., Liu, L., Li, Y., Cao, Z., Chen, M., Chen, Z., Chen, H. et al. (2016). LPS/TLR4 signaling enhances TGF-β response through downregulating BAMBI during prostatic hyperplasia. *Sci. Rep.* **6**, 27051.

Higgins, D. F., Kimura, K., Iwano, M. and Haase, V. H. (2008). Hypoxia-inducible factor signaling in the development of tissue fibrosis. *Cell Cycle* **7**, 1128-1132.

Hung, S.-P., Yang, M.-H., Tseng, K.-F. and Lee, O. K. (2013). Hypoxia-induced secretion of TGF-β1 in mesenchymal stem cell promotes breast cancer cell progression. *Cell Transplant.* **22**, 1869-1882.

Jiang, J., Tang, Y.-L. and Liang, X.-H. (2011). EMT: A new vision of hypoxia promoting cancer progression. *Cancer. Biol. Ther.* **11**, 714-723.

Jovanović, B., Pickup, M. W., Chytil, A., Gorska, A. E., Johnson, K. C., Moses, H. L. and Owens, P. (2016). TβRIII expression in human breast cancer stroma and the role of soluble TβRIII in breast cancer associated fibroblasts. *Cancers* **8**, E100.

Kaelin, W. G., Jr and Ratcliffe, P. J. (2008). Oxygen sensing by metazoans: the central role of the HIF hydroxylase pathway. *Mol. Cell* **30**, 393-402.

Kalluri, R. and Weinberg, R. A. (2009). The basics of epithelial-mesenchymal transition. *J. Clin. Invest.* **119**, 1420-1428.

Keith, B., Johnson, R. S. and Simon, M. C. (2011). HIF1α and HIF2α: Sibling rivalry in hypoxic tumour growth and progression. *Nat. Rev. Cancer.* **12**, 9-22.

Koh, M. Y. and Powis, G. (2012). Passing the baton: the HIF switch. *Trends Biochem. Sci.* **37**, 364-372.

Manninen, A., Verkade, P., Le Lay, S., Torkko, J., Kasper, M., Fullekrug, J. and Simons, K. (2005). Caveolin-1 is not essential for biosynthetic apical membrane transport. *Mol. Cell. Biol.* **25**, 10087-10096.

Marwitz, S., Depner, S., Dvornikov, D., Merkle, R., Szczygiel, M., Müller-Decker, K., Lucarelli, P., Wäsch, M., Mairbäurl, H., Rabe, K. F. et al. (2016). Downregulation of the TGF-β pseudoreceptor BAMBI in non-small cell lung cancer enhances TGF-β signaling and invasion. *Cancer Res.* **76**, 3785-3801.

Massagué, J. (2012). TGFβ signalling in context. *Nat. Rev. Mol. Cell Biol.* **13**, 616-630.

Massagué, J. and Gomis, R. R. (2006). The logic of TGFβ signaling. *FEBS Lett.* **580**, 2811-2820.

Massagué, J., Seoane, J. and Wotton, D. (2005). Smad transcription factors. *Genes Dev.* **19**, 2783-2810.

Meade, E. S., Ma, Y. Y. and Guller, S. (2007). Role of hypoxia-inducible transcription factors 1α and 2α in the regulation of plasminogen activator inhibitor-1 expression in a human trophoblast cell line. *Placenta* **28**, 1012-1019.

Myllyharju, J. (2013). Prolyl 4-hydroxylases, master regulators of the hypoxia response. *Acta Physiol.* **208**, 148-165.

Myllymäki, S. M., Teräväinen, T. P. and Manninen, A. (2011). Two distinct integrin-mediated mechanisms contribute to apical lumen formation in epithelial cells. *PLoS ONE* **6**, e19453.

Onichtchouk, D., Chen, Y.-G., Dosch, R., Gawantka, V., Delius, H., Massagué, J. and Niehrs, C. (1999). Silencing of TGF-β signalling by the pseudoreceptor BAMBI. *Nature* **401**, 480-485.

Poellinger, L. and Lendahl, U. (2008). Modulating Notch signaling by pathway-intrinsic and pathway-extrinsic mechanisms. *Curr. Opin. Genet. Dev.* **18**, 449-454.

Ran, F. A., Hsu, P. D., Wright, J., Agarwala, V., Scott, D. A. and Zhang, F. (2013). Genome engineering using the CRISPR-Cas9 system. *Nat. Protoc.* **8**, 2281-2308.

Rankin, E. B. and Giaccia, A. J. (2016). Hypoxic control of metastasis. *Science* **352**, 175-180.

Robertson, I. B. and Rifkin, D. B. (2013). Unchaining the beast; insights from structural and evolutionary studies on TGFβ secretion, sequestration, and activation. *Cytokine Growth Factor. Rev.* **24**, 355-372.

Ruthenborg, R. J., Ban, J.-J., Wazir, A., Takeda, N. and Kim, J.-W. (2014). Regulation of wound healing and fibrosis by hypoxia and hypoxia-inducible factor-1. *Mol. Cells* **37**, 637-643.

Sahlgren, C., Gustafsson, M. V., Jin, S., Poellinger, L. and Lendahl, U. (2008). Notch signaling mediates hypoxia-induced tumor cell migration and invasion. *Proc. Natl. Acad. Sci. USA* **105**, 6392-6397.

Sakamoto, T., Weng, J. S., Hara, T., Yoshino, S., Kozuka-Hata, H., Oyama, M. and Seiki, M. (2014). Hypoxia-inducible factor 1 regulation through cross talk between mTOR and MT1-MMP. *Mol. Cell. Biol.* **34**, 30-42.

Sánchez-Elsner, T., Botella, L. M., Velasco, B., Corbí, A., Attisano, L. and Bernabéu, C. (2001). Synergistic cooperation between hypoxia and transforming growth factor-β pathways on human vascular endothelial growth factor gene expression. *J. Biol. Chem.* **276**, 38527-38535.

Sasaki, T., Sasahira, T., Shimura, H., Ikeda, S. and Kuniyasu, H. (2004). Effect of nma on growth inhibition by TGF-βa in human gastric carcinoma cell lines. *Oncol. Rep.* **11**, 1219-1223.

Schäffer, L., Scheid, A., Spielmann, P., Breymann, C., Zimmermann, R., Meuli, M., Gassmann, M., Marti, H. H. and Wenger, R. H. (2003). Oxygen-regulated

expression of TGF-β3, a growth factor involved in trophoblast differentiation. *Placenta* **24**, 941-950.

Schödel, J., Mole, D. R. and Ratcliffe, P. J. (2013). Pan-genomic binding of hypoxia-inducible transcription factors. *Biol. Chem.* **394**, 507-517.

Schuck, S., Manninen, A., Honsho, M., Füllekrug, J. and Simons, K. (2004). Generation of single and double knockdowns in polarized epithelial cells by retrovirus-mediated RNA interference. *Proc. Natl. Acad. Sci. USA* **101**, 4912-4917.

Semenza, G. L. (2012). Hypoxia-inducible factors in physiology and medicine. *Cell* **148**, 399-408.

Shalem, O., Sanjana, N. E., Hartenian, E., Shi, X., Scott, D. A., Mikkelsen, T. S., Heckl, D., Ebert, B. L., Root, D. E., Doench, J. G. et al. (2014). Genome-scale CRISPR-Cas9 knockout screening in human cells. *Science* **343**, 84-87.

Suzuki, T., Shinjo, S., Arai, T., Kanai, M. and Goda, N. (2014). Hypoxia and fatty liver. *World J. Gastroenterol.* **20**, 15087-15097.

Teräväinen, T. P., Myllymäki, S. M., Friedrichs, J., Strohmeyer, N., Moyano, J. V., Wu, C., Matlin, K. S., Muller, D. J. and Manninen, A. (2013). αV-integrins are required for mechanotransduction in MDCK epithelial cells. *PLoS ONE* **8**, e71485.

Tsang, M., Kim, R., de Caestecker, M. P., Kudoh, T., Roberts, A. B. and Dawid, I. B. (2000). Zebrafish nma is involved in TGFβ family signaling. *Genesis* **28**, 47-57.

Vaupel, P. and Mayer, A. (2007). Hypoxia in cancer: significance and impact on clinical outcome. *Cancer Metastasis Rev.* **26**, 225-239.

Wipff, P. J. and Hinz, B. (2008). Integrins and the activation of latent transforming growth factor β1 - an intimate relationship. *Eur. J. Cell Biol.* **87**, 601-615.

Zhang, J. C., Chen, G., Chen, L., Meng, Z. J., Xiong, X. Z., Liu, H. J., Jin, Y., Tao, X. N., Wu, J. H. and Sun, S. W. (2016). TGF-β/BAMBI pathway dysfunction contributes to peripheral Th17/treg imbalance in chronic obstructive pulmonary disease. *Sci. Rep.* **6**, 31911.

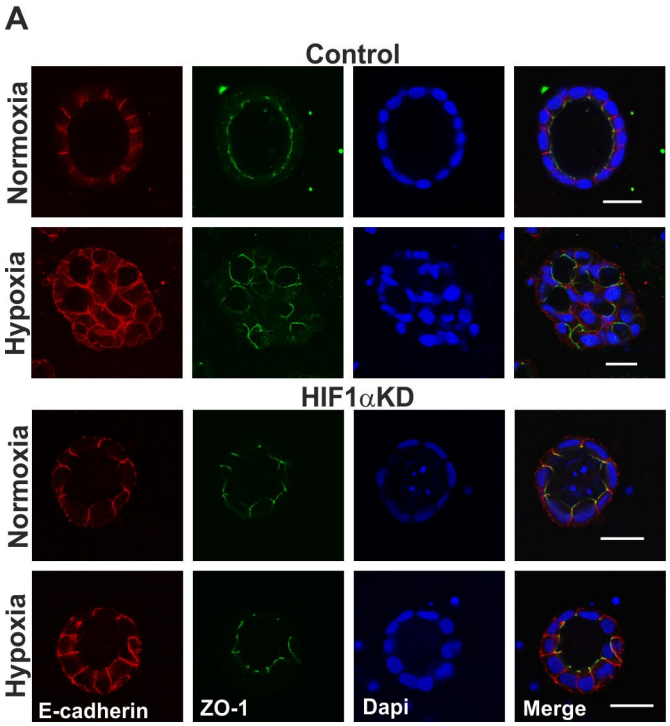

Figure S1. **Knockdown of HIF1α does not affect subapical localization of a tight junction marker ZO-1.** (A) Control and HIF1α-KD MDCK cysts were grown in normoxic or hypoxic (1% O_2) conditions in 3D BME gels for 6 days, fixed and stained for ZO-1 (green), E-cadherin (red) and nuclei (DAPI, blue). A single confocal slice from the middle of the cysts is shown. Scale bars are 20 μm.

Journal of Cell Science • Supplementary information

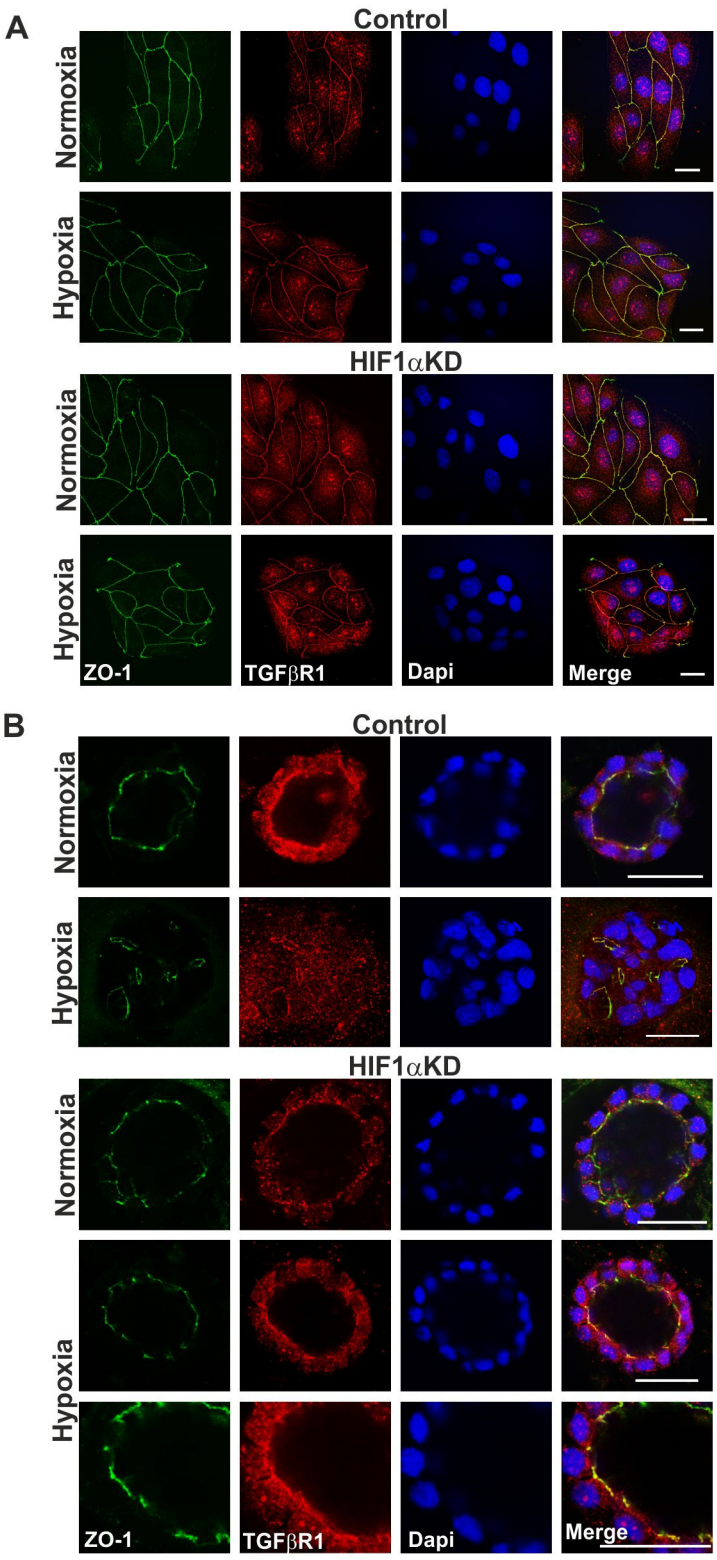

Figure S2. **Knockdown of HIF1α does not affect ZO-1 or TGFβR1 co-localization at subapical tight junctions.** (A) Control and HIF1α-KD MDCK cysts were grown in normoxic or hypoxic (1% O_2) conditions as 2D cultures on glass coverslips for 24 h, or as (B) 3D cultures in BME gels for 6 days, fixed and stained for ZO-1 (green), TGFβR1 (red) and nuclei (DAPI, blue). A single confocal slice from (A) subapical region in MDCK cell monolayer or (B) the middle of the MDCK cyst is shown. Scale bars are 20 μm.

Journal of Cell Science • Supplementary information

SUPPLEMENTARY TABLES

Table S1. shRNA target sequences used in the study and their respective mRNA depletion efficiencies

Construct	Target sequence(a)	%mRNA(b)	Number of samples
HIF1αKD#1	GCTGGAGACACAATCATATCT	73.6±6.7	11
HIF1αKD#2	GCGAGCACAATTACAGTATTC	64.8±8.6	11
HIF1αKD#3	GCTGAAGACACAGAAGCAAAG	94.6±2.5	11

[a]Target sequences were cloned into Retroviral RVH1-puro shRNA vectors as described previously (Schuck et al., 2004).

[b]Indicated as the percent decrease in mRNA level (relative to TBP) in comparison to control samples.

Table S2. sgRNA target sequences used in the study.

Construct	Target sequence(s)
BambiKO#1	GCTGCCCACTGCGTGGCAAC
BambiKO#2	GCTGTGATGCTGCCCACTGCG

[a]Target sequences were cloned into lentiCRISPRv1vector as described previously (Shalem et al., 2014).

Journal of Cell Science • Supplementary information

Table S3. Verification of gene editing by sequencing of the edited genome region.

Construct BambiKO#1	Sequencing result	Editing
Bambi WT 1 both alleles	GCTGCCCACTGCGTGGCAAC	
BambiKO#1		
Allele 1	GCTGCCCACTGCGTGGCA-CTGGTTATATGTGTAAATCTGAGCTGA	-1bp
Allele 2	GCTGCCCACTGCGTGGCA-CTGGTTATATGTGTAAATCTGAGCTGA	-1bp
Construct BambiKO#2		
Bambi WT 2 both alleles	GCTGTGATGCTGCCCACTGCG	
BambiKO#2		
Allele 1	ACTGTGATGCTGCCCACTTGCGTGGCAACTGGTTATATGTGTAA	+1bp
Allele 2	ACTGTGATGCTGCCCA----------ACTGGTTATATGTGTAAATCTGAGCTGA	-10bp

Deletion is marked by -, insertion is marked in yellow, stop codon is marked in grey.

Journal of Cell Science • Supplementary information

Table S4. Oligonucleotides used for PCR and qRT-PCR analyses.

canis HIF1a F	cgtgcttggtgctgatttgt
canis HIF1a R	ggtcagagtccaaagcatga
canis ADM F	cttcgagtgtccagcagcta
canis ADM R	cggtagcgtttgactcggat
canis ALDOC F	ggaggcatcactcaacctca
canis ALDOC R	acctcagcccgcttgatgaa
canis BNIP3 F	ccgagcttcggaagtagaca
canis BNIP3 R	gccgacttgaccaatcccaa
canis BNIP3L F	agcgtttgggatgtctgaag
canis BNIP3L R	gtgtgctcagtcgctttcca
canis VEGFA F	gtgcattggagccttgcctt
canis VEGFA R	tgtactcgatctcgtcaggg
canis LOX F	ctccgacgacaacccctatt
canis LOX R	gtggacgcctggatgtagta
canis SNAI1 F	gatgcacatccgaagccaca
canis SNAI1 R	gggaacaggtcttgcactga
canis SNAI2 F	gggcgcccttaaaatgcaca
canis SNAI2 R	ctgcagatgagccctcagat
canis ZEB1 F	ccaggtggcttacacgtact
canis ZEB1 R	gggtggtgtagaatcagagtca
canis CDH1 F	ccaggcagtcttccaaggat
canis CDH1 R	cacgctgatgactcctgtgt
canis VIM F	gcgtgatgtacgccagcaat
canis VIM R	cacctgtctccggtactcat
canis Smad2 F	gggaatcgagccacagagta
canis Smad2 R	ctcgccaaccctctggttta
canis Smad3 F	ggcggtcaagagtttggtca
canis Smad3 R	gcagacctcgtccttcttca
canis Smad4 F	tgccatagacaaggtggaga
canis Smad4 R	cctccagagacgagcataga

Journal of Cell Science • Supplementary information

canis Smad7 F	ttactccagatacccgatgg
canis Smad7 R	caggctccagaagaagttgg
canis TGFβ1 F	ggccaccattcatggcatga
canis TGFβ1 R	cgtgtccaggctccaaatgt
canis TGFβ2 F	gccctcctacagacttgagt
canis TGFβ2 R	ccacccaagatccctcttga
canis TGFβ3 F	cgctatatcggcggcaagaa
canis TGFβ3 R	ggatgtctccattgggctga
canis TGFβR1 F	ctgccataaccgtaccgtca
canis TGFβR1 R	ctctccactttcctcgccaa
canis TGFβR2 F	gcctgtgtgactttggcctt
canis TGFβR2 R	cccactgcattacagcgaga
canis TGFβR3 F	ccctgaatggctgtggtact
canis TGFβR3 R	caggtcggctgaagaaggaa
canis LTBP1 F	gcagctgtcagaacagctgt
canis LTBP1 R	ccatggactgggatctgaca
canis LTBP4 F	cctggagggcgatttctgtt
canis LTBP4 R	ccgtcggtgttggtacagat
canis CDKN1A F	c gggagcgatg gaactttga
canis CDKN1A R	gggcttcctcttggagaaga
canis CDC25A F	gcgagc cagggaatttcctt
canis CDC25A R	cagaggcttgccatgcatga
canis PAI1 F	ggagagacttgtcggcagat
canis PAI1 R	gccgtgaaccagcttcagat
canis BAMBI F	ggatcgccattccagctaca
canis BAMBI R	cagtgggcagcatcacagta

Journal of Cell Science • Supplementary information